Available online at www.sciencedirect.com

ScienceDirect

Procedia Materials Science 4 (2014) 311 – 316

Procedia Materials Science

www.elsevier.com/locate/procedia

8th International Conference on Porous Metals and Metallic Foams, Metfoam 2013

Characterization of polymer-metal foam hybrids for use in vibration dampening and isolation

Shunjie Yin , Nassif Rayess *

Department of Mechanical Engineering, University of Detroit Mercy, Detroit, MI 48221, USA

Abstract

There is an ever-increasing demand for lightweight, multifunctional material having both higher stiffness and higher damping. In many applications, higher damping in isolators can allow for beneficial changes in the natural frequencies of the vibration isolation system without deterioration in performance. Generally, simplex materials with higher damping usually have lower stiffness and vice versa. This trade-off limits the applicability of homogenous materials in such roles. Therefore, a hybrid material consisting of open cell aluminum foam as 'skeleton' with polymeric material introduced into the open pores could be designed to better meet these contradictory demands. This study aims to characterize the dynamic and damping properties of the composite of the aluminum foam and polymer. The hybrid material, modeled as a single degree-of-freedom spring-damper system, is loaded under a sinusoidal compressive force using a universal testing machine yielding a measure of the dynamic stiffness and damping coefficient. This paper presents the experimentally measured damping characteristics for both the unaltered foam as well as the various hybrids of polymers and aluminum foams. By modeling the hybrid as parallel springs of the aluminum and polymers, the damping due to the interface between the two materials is quantified and presented.

Peer-review under responsibility of Scientific Committee of North Carolina State University

Keywords: Composite; Vibration; Dampening; Stiffness; Interface property; Characterization methods.

1. Introduction

The use of open cell foam in vibration isolation and sound absorption involves the introduction of polymeric materials into the voids of the foam, principally foams and rubbers (Imam et al. (1999), Rahul et al. (2009)). Such an addition of the filler material provides added functionality that is not provided by the metal foam. In cases where

* Corresponding author. Tel.: 313-993-1402;.fax: 313-993-1187
E-mail address: rayesna@udmercy.edu

Peer-review under responsibility of Scientific Committee of North Carolina State University
doi:10.1016/j.mspro.2014.07.564

the added filler is a high damping material such as polymer foam or elastomeric material, the result could be added damping at relatively high stiffness.

The interface between the metal foam and the rubber plays a significant role both in the damping and the stiffness of the composite material. As the interface properties cannot be directly measured, this article provides the framework for an indirect measurement and gives some preliminary results.

2. Experimental Approach

2.1. Aluminum Foam/Elastomer Composite

The aluminum foam/elastomer composite is fabricated by shaping a 10 PPI Duocel® aluminum foam and filling the open pores with elastomeric resins. In this study, a two part Silicon rubber and an RTV rubber were used. A close-up of the material is shown in Figure 1.

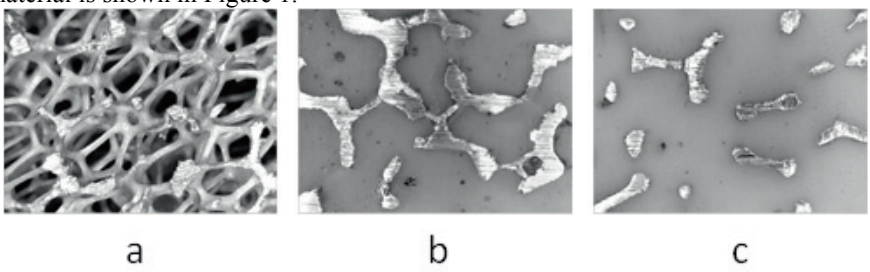

Fig. 1. Close-up view of the aluminum foam/elastomer composite: a) Aluminum foam only. b) With Silicon rubber. c) With RTV.

2.2. Theoretical Framework

For the purpose of this analysis, the aluminum foam and rubber are assumed to be parallel spring/damper systems, denoted in Figure 2 by the subscripts "*F*" and "*R*", respectively. The interface between the rubber and the aluminum is also modeled as a spring/damper system in parallel and denoted by the subscript "*I*".

Referring to Figure 2, the metal foam and rubber system undergoes an imposed sinusoidal deformation δ, given by

$$\delta = \Delta e^{i\omega t} \tag{1}$$

where Δ is the amplitude of oscillations, ω is the circular frequency in radians/sec and t is the time.

The deformation δ corresponds to a sinusoidal force F_T, given by

$$F_T = F_{oT} e^{i(\omega t - \varnothing)} \tag{2}$$

where F_{oT} is the amplitude of the force and ϕ is the phase angle between the force and deformation in the sample.

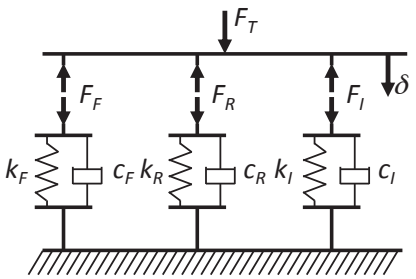

Fig. 2. Model of rubber, aluminum and the interface between the two, denoted by the subscripts "*F*", "*R*" and "*I*", respectively.

The force F_T is borne by the aluminium foam (force F_F), rubber (F_R) and the interface (F_I), in the following manner

$$F_T = F_F + F_R + F_I \tag{3}$$

Forces F_T, F_F, F_R and F_I are related to the stiffness and damping of the respective materials by

$$F_{T,F,R,I} = k_{T,F,R,I}\delta + c_{T,F,R,I}\dot{\delta} = \left(k_{T,F,R,I} + i\omega c_{T,F,R,I}\right)\delta \tag{4}$$

where $\dot{\delta}$ is the time derivative of the displacement and the term $\left(k_{T,F,R,I} + i\omega c_{T,F,R,I}\right)$ is the complex stiffness and is denoted by $K_{T,F,R,I}$.

The complex stiffness can be related to the material loss factor η by

$$K_{T,F,R,I} = k_{T,F,R,I}\left(1 + i\frac{\omega c_{T,F,R,I}}{k_{T,F,R,I}}\right) = k_{T,F,R,I}\left(1 + i\eta_{T,F,R,I}\right). \tag{5}$$

The material loss factor is related to tangent of the phase angle ϕ given in Equation 2 by

$$\eta_{T,F,R,I} = tan\left(\phi\right). \tag{6}$$

Referring to Equations 3, the total dynamic stiffness K_T of the composite material is related to the dynamic stiffness of the unit materials by

$$K_T = K_F + K_R + K_I, \tag{7}$$

which can be combined with Equation 5 to yield

$$k_T\left(1 + i\eta_T\right) = k_F\left(1 + i\eta_F\right) + k_R\left(1 + i\eta_R\right) + k_I\left(1 + i\eta_I\right) \tag{8}$$

and consequently, the total loss factor η_T is given by

$$\eta_T = \eta_F\frac{k_F}{k_T} + \eta_R\frac{k_R}{k_T} + \eta_I\frac{k_I}{k_T} \tag{9}$$

The frequency dependent dynamic stiffness of the material is obtained by substituting Equations 1 and 2 into equation 4 and writing it in term of the complex stiffness given in 5, yielding

$$F_{oT}e^{i(\omega t - \varnothing)} = k_T\left(1 + i\eta_T\right)\Delta e^{i\omega t} \tag{10}$$

which can be combined with Equation 9 to yield

$$\frac{F_{oT}}{\Delta} = \begin{bmatrix}\left(k_F + k_R + k_I\right) + \\ i\left(\eta_F k_F + \eta_R k_R + \eta_I k_I\right)\end{bmatrix} e^{i\phi} \tag{11}$$

which amplitude can be written as

$$\left|\frac{F_{oT}}{\Delta}\right|^2 = \left(k_F + k_R + k_I\right)^2 + \left(\eta_F k_F + \eta_R k_R + \eta_I k_I\right)^2 \tag{12}$$

3. Measurement Scheme

In order to make use of Equations 9 and 12, the static stiffness of the rubber k_R, aluminum foam k_F and composite k_T, are directly quantified from the slope of the stress-strain curves. The dynamic stiffness of the composite $|F_{oT}/\Delta|$ and the loss factor of the rubber η_R, aluminum foam η_F and composite η_T, are frequency dependent and are measured using the transfer function technique. That leaves the interface stiffness k_I and damping loss factor η_I as the only parameters that cannot be directly measured but can be deduced from solving Equations 9 and 12 simultaneously. Doing so, yields

$$k_I = \sqrt{\left|\frac{F_{oT}}{\Delta}\right|^2 - \left(\eta_T k_T\right)^2} - k_F - k_R \tag{13}$$

and

$$\eta_I = \frac{\eta_T k_T - \eta_F k_F - \eta_R k_R}{k_I} \tag{14}$$

The force and deformation are measured in the time domain as F(t) and δ(t), given by $F(t) = F_o e^{i(\omega t - \phi_F)}$ and $\delta(t) = \Delta e^{i(\omega t - \phi_\delta)}$, respectively. The Fourier Transform of the two signals, given by $F(\omega)$ and $\delta(\omega)$ are calculated using the LabView Software and given by $F(\omega) = F_o e^{-i\phi_F}$ and $\delta(\omega) = \Delta e^{-i\phi_\delta}$. The transfer function, given by

$$\frac{F(\omega)}{\delta(\omega)} = \frac{F_o}{\Delta} e^{-i(\phi_F - \phi_\delta)} \tag{15}$$

The term F_o/Δ is the dynamic stiffness and the term $(\phi_F - \phi_\delta)$ is the phase angle, the tangent of which is the loss factor used in Equation 6.

4. Test Setup

The test setup involves dynamic compression of a test specimen (1 inch square cylinder with 1.35 inch tall, shown in Figure 3). The specimen are capped with a low melting temperature Bismuth alloy in order to provide parallel and smooth loading surfaces.

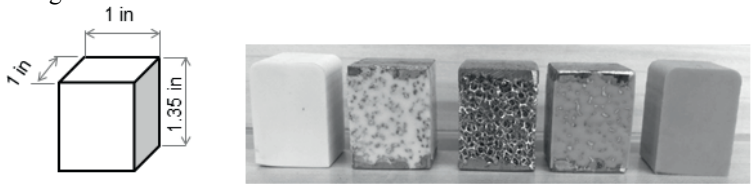

Fig. 3. From right to left: Silicon rubber specimen, Silicon rubber/aluminum foam composite, aluminum foam only, RTV/aluminum foam composite, RTV only and a schematic of the test specimen.

The test specimen is loaded in compression on a modified test frame shown in Figures 4 and 5. A custom-built extensometer system is employed to directly measure the specimen deformation.

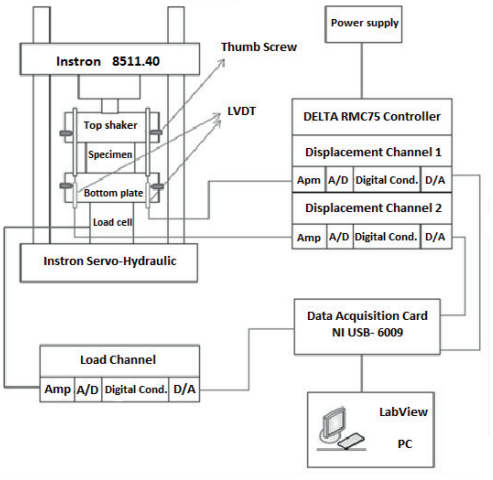

Fig. 4. Schematic of the dynamic compression test setup.

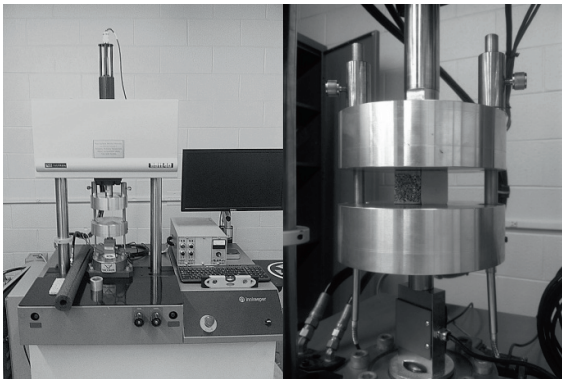

Fig. 5. Photo of test setup. Close-up of fixture on the right.

5. Results and Discussion

In this preliminary result article, three groups of samples for each material were made and tested. Each group consists of three specimen of aluminum foam machined from the same block after the Bismuth alloy layer was introduced. The groups of samples were sequestered because the size of the Bismuth alloy layer that forms the caps of the sample was found to affect the measured characteristics. Of the three identical aluminum foam specimen, one was kept intact and the other two were filled with the Silicon and the RTV rubbers.

The three groups of samples were tested at 1 Hz and 2 Hz and with a mean loading of 50 lbs and a double-amplitude of 50 lbs. The measured static stiffness is given in TABLE 1. The measured dynamic stiffness and corresponding loss factors are given in TABLE 2 and TABLE 3 for the aluminum foam and for the two composites and these were obtained using Equations 15 and 6, respectively.

The dynamic test data is an average of ten measurements taken on the same sample in various positions to reduce the manufacturing errors and repeat measurement errors.

Table 1. Measured static stiffness for aluminum foam, aluminum foam/silicon rubber composite and aluminum foam/RTV rubber composite, silicone rubber and RTV rubber.

MEASURED STATIC STIFFNESS (KN/M)			
Materials	Group 1	Group 2	Group 3
Al Foam	5454.3	5371.7	4147.7
AF/Silicone Composite	6868.0	5459.1	4572.4
AF/RTV Composite	6301.4	5787.8	5102.1
Silicone		18.9	
RTV		37.0	

Table 2. Measured dynamic stiffness for aluminum foam, aluminum foam/silicon rubber composite and aluminum foam/RTV rubber composite at 1 and 2 Hz.

MEASURED DYNAMIC STIFFNESS (KN/M)						
Materials	Group 1		Group 2		Group 3	
	1Hz	2Hz	1Hz	2Hz	1Hz	2Hz
Al Foam	5383.0	5050.3	5496.9	5380.9	4353.7	4083.8
AF/silicone	5994.9	5706.9	5809.9	5696.0	4723.2	4514.2
AF/RTV	6680.6	6626.3	6385.6	6175.0	5450.6	5269.0

Table 3. Measured loss factor for aluminum foam, aluminum foam/silicon rubber composite and aluminum foam/RTV rubber composite at 1 and 2 Hz

MEASURED LOSS FACTOR						
Materials	Group 1		Group 2		Group 3	
	1Hz	2Hz	1Hz	2Hz	1Hz	2Hz
Al Foam	0.0093	0.0139	0.0113	0.0152	0.0125	0.0177
AF/silicone	0.0109	0.0164	0.0137	0.0181	0.0158	0.0211
AF/RTV	0.0126	0.0169	0.0149	0.0195	0.0177	0.0238

The results shown in TABLES 1, 2 and 3 reveal that the addition of the rubber caused a general increase in both the static stiffness and in the dynamic stiffness as well as a general increase in the loss factor.

The observed increase in the stiffness and damping of the interpenetrating composite (rubber and foam) is found to be far larger (nearly twenty fold increase in stiffness) than the added effect of the two materials taken separately. From a physics perspective, this large increase can be explained by the rubber's strong aversion to volumetric change. The rubber, being trapped between the aluminum ligaments, gives rise to bearing reactions that limits the deformation of the ligaments under load. The mathematical embodiment of this phenomenon takes the form of an interface stiffness and damping given by Equations 8 and 9.

The interface stiffness and loss factor for the aluminum foam/rubber composites, calculated using Equations 13 and 14, are shown in TABLE 4 and 5.

Table 4. Calculated interface stiffness for aluminum foam/silicon rubber composite and aluminum foam/RTV rubber composite at 1 and 2 Hz

CALCULATED INTERFACE STIFFNESS (KN/M)						
Materials	Group 1		Group 2		Group 3	
	1Hz	2Hz	1Hz	2Hz	1Hz	2Hz
AF/silicone	521.4	232.7	418.7	304.5	538.3	346.6
AF/RTV	1188.9	1116.6	976.5	765.5	1265.3	1083.0

TABLE 6 shows the average percent increase in dynamic stiffness and loss factor with the introduction of the two types of rubber into the aluminium foam. The harder RTV rubber resulted in higher increases in both dynamic stiffness and loss factor over the softer Silicon rubber.

Table 5. Calculated interface loss factor for aluminum foam/silicon rubber composite and aluminum foam/RTV rubber composite at 1 and 2 Hz

CALCULATED INTERFACE STIFFNESS (KN/M)						
Materials	Group 1		Group 2		Group 3	
	1Hz	2Hz	1Hz	2Hz	1Hz	2Hz
AF/silicone	.0238	.0832	.0317	.0529	.0364	.0635
AF/RTV	.0205	.0205	.0244	.0385	.0290	.0418

Table 6. The average increase percentage for three groups in stiffness and loss factor of the composites compared with the unfilled aluminum foams.

THE AVERAGE PERCENT INCREASE					
	Static Testing	Dynamic Testing			
Materials	Stiffness	Dynamic stiffness		Loss Factor	
		1Hz	2Hz	1Hz	2Hz
AF/Silicone	6.5%	8.4%	9.8%	19.9%	18.8%
AF/RTV	15.4%	21.8%	26.4%	31.7%	28.1%

6. Conclusions

An aluminium foam/rubber composite is made by filling the void of the foam with liquid rubber. Upon curing, the composite is tested under cyclical compressive loading and is shown to have a significant increase both in damping loss factor and dynamic stiffness over the aluminium foam only. The effect of the combined material (rubber inside the aluminium foam) is found to be an order of magnitude larger than the effect of the two materials side by side. This effect is explained by the rubber's strong aversion to volumetric change after being confined inside the cells of the aluminium foam.

References

J. Rahul and T. Hareesh. 2009. "Processing, Compression Response and Finite Element Modeling of Syntactic Foam Based Interpenetrating Phase Composite (IPC)." Materials Science and Engineering: A 499 (1-2) (January): 507-517.

M.A. Imam, S.B. Sastri, and T.M. Keller. 1999. "Lightweight High Damping Porous Metal/Phthalonitrile Composites." U.S. Patent 5,895,726.